

Title	Exciton localization in semipolar (112 ⁻²) InGaN multiple quantum wells
Authors	Dinh, Duc V.;Brunner, Frank;Weyers, Markus;Corbett, Brian M.;Parbrook, Peter J.
Publication date	2016-08-04
Original Citation	Dinh, D. V., Brunner, F., Weyers, M., Corbett, B. and Parbrook, P. J. (2016) 'Exciton localization in semipolar (112 ⁻²) InGaN multiple quantum wells', Journal of Applied Physics, 120(5), 055705. doi:10.1063/1.4960348
Type of publication	Article (peer-reviewed)
Link to publisher's version	10.1063/1.4960348
Rights	© 2016, AIP Publishing. This article may be downloaded for personal use only. Any other use requires prior permission of the author and AIP Publishing. The following article appeared in Journal of Applied Physics 120, 055705 (2016) and may be found at http://aip.scitation.org/doi/abs/10.1063/1.4960348
Download date	2025-08-01 10:08:48
Item downloaded from	https://hdl.handle.net/10468/4203



UCC

University College Cork, Ireland
Coláiste na hOllscoile Corcaigh

Exciton localization in semipolar ($1\bar{1}\bar{2}2$) InGaN multiple quantum wells

Duc V. Dinh^{*}, F. Brunner, M. Weyers, B. Corbett, and P. J. Parbrook

Citation: *Journal of Applied Physics* **120**, 055705 (2016); doi: 10.1063/1.4960348

View online: <http://dx.doi.org/10.1063/1.4960348>

View Table of Contents: <http://aip.scitation.org/toc/jap/120/5>

Published by the American Institute of Physics

Articles you may be interested in

[Role of substrate quality on the performance of semipolar \(\$1\bar{1}\bar{2}2\$ \) InGaN light-emitting diodes](#)

Journal of Applied Physics **120**, 135701 (2016); 10.1063/1.4963757

[Radiative recombination mechanisms in polar and non-polar InGaN/GaN quantum well LED structures](#)

Applied Physics Letters **109**, 151110 (2016); 10.1063/1.4964842

[Temperature-dependent recombination coefficients in InGaN light-emitting diodes: Hole localization, Auger processes, and the green gap](#)

Applied Physics Letters **109**, 161103 (2016); 10.1063/1.4965298

[Theoretical and experimental analysis of the photoluminescence and photoluminescence excitation spectroscopy spectra of m-plane InGaN/GaN quantum wells](#)

Applied Physics Letters **109**, 223102 (2016); 10.1063/1.4968591

[Stimulated emission via electron-hole plasma recombination in fully strained single InGaN/GaN heterostructures](#)

Applied Physics Letters **109**, 221106 (2016); 10.1063/1.4968799

[III-Nitride-on-silicon microdisk lasers from the blue to the deep ultra-violet](#)

Applied Physics Letters **109**, 231101 (2016); 10.1063/1.4971357

AIP | Journal of
Applied Physics

Save your money for your research.

It's now **FREE** to publish with us -

no page, color or publication charges apply.

Publish your research in the
Journal of Applied Physics
to claim your place in applied
physics history.

Exciton localization in semipolar (11 $\bar{2}$ 2) InGa \bar{N} multiple quantum wells

Duc V. Dinh,^{1,a)} F. Brunner,² M. Weyers,² B. Corbett,¹ and P. J. Parbrook^{1,3}

¹Tyndall National Institute, University College Cork, Lee Matlings, Dyke Parade, Cork, Ireland

²Ferdinand-Braun-Institut, Leibniz-Institut für Höchstfrequenztechnik, Gustav-Kirchhoff-Str. 4, 12489 Berlin, Germany

³School of Engineering, University College Cork, Cork, Ireland

(Received 1 July 2016; accepted 21 July 2016; published online 4 August 2016)

The exciton localization in semipolar (11 $\bar{2}$ 2) In $_x$ Ga $_{1-x}$ N ($0.13 \leq x \leq 0.35$) multiple-quantum-well (MQW) structures has been studied by excitation power density and temperature dependent photoluminescence. A strong exciton localization was found in the samples with a linear dependence with In-content and emission energy, consistent with the Stokes-shift values. This strong localization was found to cause a blue-shift of the MQW exciton emission energy at temperature above 100 K, which was found to linearly increase with increasing In-content. *Published by AIP Publishing.* [<http://dx.doi.org/10.1063/1.4960348>]

I. INTRODUCTION

The major achievements in InGa \bar{N} quantum-well (QW) active region based light-emitting diodes (LEDs) have mainly been made on the (0001) polar surface.¹ However, this surface has a disadvantage, namely, the quantum-confined Stark effect (QCSE) caused by polarization induced electrostatic fields.^{2,3} This QCSE causes a strong spatial separation of electron and hole wave-functions resulting in low radiative recombination rates, which consequently reduce the internal quantum efficiency (IQE). The strength of QCSE becomes significant with increasing In-content due to the increased InGa \bar{N} /Ga \bar{N} lattice mismatch reducing the IQE at longer emission wavelengths, particularly in the green and yellow spectral regions. Additionally, this QCSE also causes a blue-shifted emission energy with an increase in excitation power density due to the reduction in the effective field strength by the Coulomb screening.³ To overcome these problems, one of the promising solutions is to grow InGa \bar{N} QW structures as an active region in LEDs along nonpolar and semipolar surface orientations due to a reduction in the polarization fields.^{4,5} For example, a stable photoluminescence peak energy has been observed for nonpolar a -plane (11 $\bar{2}$ 0)⁶ and m -plane (10 $\bar{1}$ 0) Al $_{0.2}$ Ga $_{0.8}$ N,⁷ irrespective of excitation power density employed. Though much research on a -plane⁸ and m -plane⁹ green InGa \bar{N} LEDs grown on bulk Ga \bar{N} substrates has been reported, the results have not yet met expectations. In contrast, high efficiency green and yellow semipolar (11 $\bar{2}$ 2) InGa \bar{N} LEDs grown on low threading dislocation density (TDD $\sim 5 \times 10^6$ cm $^{-2}$) high-cost (11 $\bar{2}$ 2) Ga \bar{N} bulk substrates have previously been demonstrated.^{10,11}

By means of time-resolved photoluminescence measurements (TR-PL), it has been experimentally reported that m -plane InGa \bar{N} ⁴ and (11 $\bar{2}$ 2) InGa \bar{N} ^{12–14} QWs have shorter recombination lifetimes compared to polar QWs. However, it should be noted that those samples show recombination dynamics identical to those observed in polar QWs. Apart from the polarization fields, another effect that can affect the recombination lifetimes is the exciton localization

(ELOC).^{2,3,15} The ELOC is derived from self-organized In-rich InGa \bar{N} regions that can prevent carriers from reaching defects. This will lead to a reduction of non-radiative recombination rates (despite the growth of QWs on high-TDD Ga \bar{N} templates) resulting in an enhanced luminescence efficiency as observed for polar QWs.^{2,15} The ELOC will cause a change in the carrier dynamics with increasing temperature resulting in an anomalous emission behaviour, namely, the S -shaped (“red-blue-red” shift) temperature dependence of QW emission energy that is usually attributed to hopping of excitons through the localized states.^{16,17} It should be noted that the ELOC intrinsically exists in InGa \bar{N} alloys, irrespective of growth orientation employed.^{2,3,11,13–15,18–21} Zhang *et al.*¹⁴ have reported that (11 $\bar{2}$ 2) QWs exhibit larger localization depths than polar QWs (estimated from TR-PL measurements at 7 K). Recently, by temperature-dependent photoluminescence (TD-PL) measurements, a strong ELOC degree has been found in (11 $\bar{2}$ 2) In $_{0.2}$ Ga $_{0.8}$ N QWs that causes a blue-shift of the QW exciton emission with rising temperature from ~ 200 K to 340 K, irrespective of excitation source used.²¹ However, so far there has been no systematic study on the ELOC in (11 $\bar{2}$ 2) In $_x$ Ga $_{1-x}$ N QWs with different In-contents using TD-PL. The most likely reason is due to the high-TDD and high basal-plane stacking fault (BSF) density Ga \bar{N} templates grown on low-cost sapphire substrates that hinder the QW growth. Within the ALIGHT project,²² we have recently developed low-TDD low-BSF-density (11 $\bar{2}$ 2) Ga \bar{N} templates grown on patterned (10 $\bar{1}$ 2) r -plane sapphire substrates (up to 100 mm diameter).²³

In this paper, by using TD-PL measurements with resonant excitation source, we systematically study on the ELOC in (11 $\bar{2}$ 2) In $_x$ Ga $_{1-x}$ N ($0.13 \leq x \leq 0.35$) multiple-quantum-well (MQW) structures grown on high quality (11 $\bar{2}$ 2) Ga \bar{N} templates on patterned r -plane sapphire substrates. Such an approach allows an exploration of general trends of the ELOC in (11 $\bar{2}$ 2) In $_x$ Ga $_{1-x}$ N MQW.

II. EXPERIMENTAL DETAILS

The MQW samples investigated in this study were grown in a 3×2 -in. Aixtron metal-organic vapour phase epitaxy (MOVPE) reactor on 6 μ m-thick (11 $\bar{2}$ 2) Ga \bar{N} templates

^{a)}Electronic email: duc.vn.dinh@gmail.com

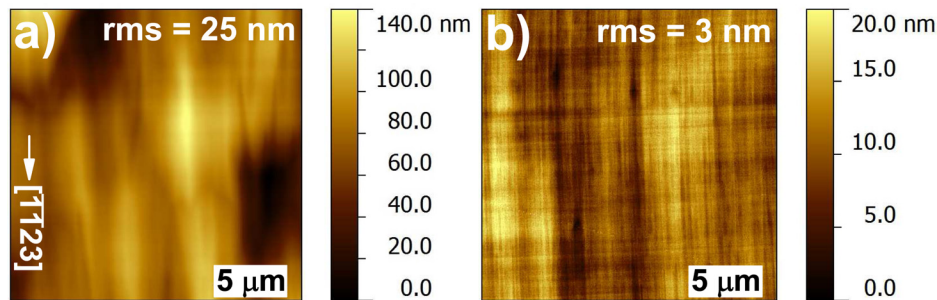


FIG. 1. AFM images ($20 \times 20 \mu\text{m}^2$) of (112̄2) InGaN MQW samples grown on (a) as-grown template and (b) CMP-template. The root-mean square (rms) roughness values of each images are shown for comparison.

that were prepared on patterned *r*-plane sapphire substrates ($\text{TDD} \sim 2 \times 10^8 \text{ cm}^{-2}$, BSF density $\sim 1 \times 10^3 \text{ cm}^{-1}$). The MOVPE growth of the templates is reported elsewhere.²³ The MQW samples consisted of a 1.5 μm -thick Si-doped GaN layer, an active MQW region consisting of five periods of InGaN/GaN with nominal 2-nm-thick wells and 10-nm-thick undoped barriers. To investigate the effect of surface morphology of the templates on the ELOC in the MQW samples, few samples were also grown on chemically mechanically polished (CMP)-templates. Details of the MQW growth procedure and CMP process are described elsewhere.²⁴ The surface morphology of the samples was investigated by Veeco MultiMode atomic force microscope (AFM) in tapping mode. The In-content of the samples was estimated using simulations based on x-ray diffraction measurements.^{21,24} To avoid the carrier diffusion problem from GaN to InGaN, TD-PL measurements of the samples have been performed using a continuous-wave violet laser diode ($E_{\text{ex}} = 3.06 \text{ eV}$) with excitation power densities (P_{ex}) of 2–15 W/cm^2 . The samples were mounted in a closed-cycle cryostat equipped with a Sumitomo (SHI) Cryogenics air-cooled compressor. The PL emission spectra were measured using a Horiba iHR320 spectrometer equipped with a monochromator and a thermoelectrically cooled Synapse CCD detector. The temperature measurements were varied from 10 K to 480 K. Additionally, PL and PL-excitation (PLE) measurements of the samples were also performed at 10 K to investigate the Stokes-shift using a monochromator coupled continuous-Xenon-lamp ($P_{\text{ex}} \sim 10^{-5} \text{ W}/\text{cm}^2$). In this case, a photomultiplier tube was used to detect the PL signal with a lock-in amplifier system.

III. RESULTS AND DISCUSSION

The typical AFM images of the MQW samples grown on as-grown and CMP-templates are shown in Fig. 1. All samples show undulated surface morphology along [11̄00]. This typical morphology has been commonly observed on nonpolar and semipolar (Al,In,Ga)N surfaces.^{6,21,24–28} This can be well explained the anisotropic diffusion of group-III atoms on these surfaces.^{26,27,29} The sample grown on a CMP template (Fig. 1(b)) shows smoother morphology with a root-mean square (rms) roughness of 3 nm for a scan size of $20 \times 20 \mu\text{m}^2$, compared to an rms value of 25 nm estimated for the sample grown on an as-grown template (Fig. 1(a)).

For example, Fig. 2(a) shows TD-PL spectra of a (112̄2) InGaN MQW sample ($x = 16\%$) grown on an as-grown template. All the spectra were fitted using a Gaussian function.

As shown in Fig. 2(b), the MQW emission energy shows a non-monotonous peak shift behaviour (i.e., an S-shaped temperature dependence), irrespective of P_{ex} used. The MQW emission energy starts to exhibit a blue-shift at above a switching temperature ($T_{R \rightarrow BL}$) of $\sim 160 \text{ K}$, then exhibits a red-shift at $T_{BL \rightarrow R} \geq 280 \text{ K}$. This can be explained via the hopping processes of excitons through the localized states.^{2,3,15–18,21} When temperature increases from 10 K to $T_{R \rightarrow BL}$, weakly localized carriers are thermally activated and they hop towards other strongly localized states resulting in the initial red-shift of emission energy. With increasing temperature from $T_{R \rightarrow BL}$ to $T_{BL \rightarrow R}$, localized carriers at lower energy levels will be strongly thermally activated to higher levels leading to the blue-shift of emission energy. Further increasing temperature above $T_{BL \rightarrow R}$, the emission energy decreases following the Varshni law as this decrease is based on thermally induced change in lattice constants and

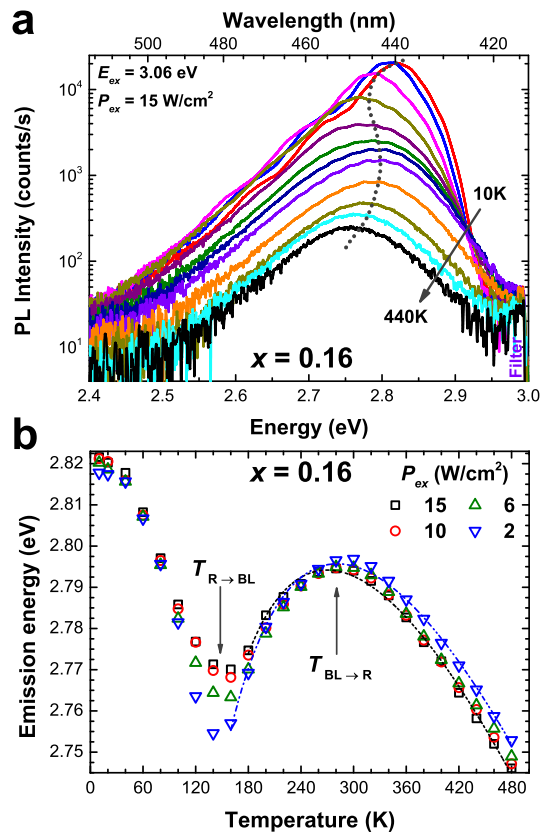


FIG. 2. (a) TD-PL spectra of a (112̄2) InGaN MQW sample ($x = 16\%$) grown on an as-grown template measured with $P_{\text{ex}} = 15 \text{ W}/\text{cm}^2$. (b) The MQW emission energy measured with different P_{ex} plotted as a function of temperature. In (b), dashed-lines are the fit to the experimental data using Eq. (1).

binding strength.³⁰ It should be noted that the sample ($x=15\%$) grown on a CMP-template also shows the same behaviour, despite the much smoother surface morphology (Fig. 1).

A similar behaviour has been found for other samples, irrespective of template used. An example can be seen in Ref. 21 for $(11\bar{2}2)$ $\text{In}_{0.2}\text{Ga}_{0.8}\text{N}$ MQW. The switching temperatures (i.e., $T_{R \rightarrow BL}$ and $T_{BL \rightarrow R}$) as a function of In-content are shown in Fig. 3. Both temperatures monotonically increase with increasing In-content indicating that the ELOC will dominate at higher temperatures.

The temperature-induced blue-shift of the MQW emission energy can be described by the Gaussian type band tail mode¹⁵

$$E_g(T) = E_g(0) - \frac{\alpha \cdot T^2}{\theta + T} - \frac{\sigma_E^2}{k_B \cdot T}, \quad (1)$$

where $E_g(0)$ is the bandgap energy of InGaN at 0 K, k_B is the Boltzmann constant, α is the Varshni fitting parameter, θ is the Debye temperature (~ 800 K for GaN). σ_E is the dispersion of the band tail, which is correlated to the ELOC degree, i.e., the larger value of σ_E means the stronger localization effect. Examples of fitted curves are shown in Fig. 2(b).

Figure 4 shows the fitted value of σ_E as a function of In-content and emission energy at 10 K. The σ_E value linearly increases from ~ 40 meV to ~ 90 meV with increasing In-content from 13% to 35%, irrespective of template used. Additionally, the σ_E values also show a linear dependence on the MQW emission energy (the inset of Fig. 4) and tend to a zero value around the GaN bandgap of 3.5 eV. This is consistent with an increased full-width at half maximum (FWHM) value of the 10 K PL spectrum with increasing In-content. For example, the 10 K FWHM values ($P_{ex} = 15$ W/cm²) were estimated to be 60 meV, 125 meV, and 180 meV for the samples with the In-content of 13% ($E_{emission} = 2.982$ eV), 30% ($E_{emission} = 2.480$ eV), and 35% ($E_{emission} = 2.285$ eV), respectively. The σ_E values are comparable irrespective of different P_{ex} used. This is consistent with the data shown in Fig. 2(b) and a previous report for

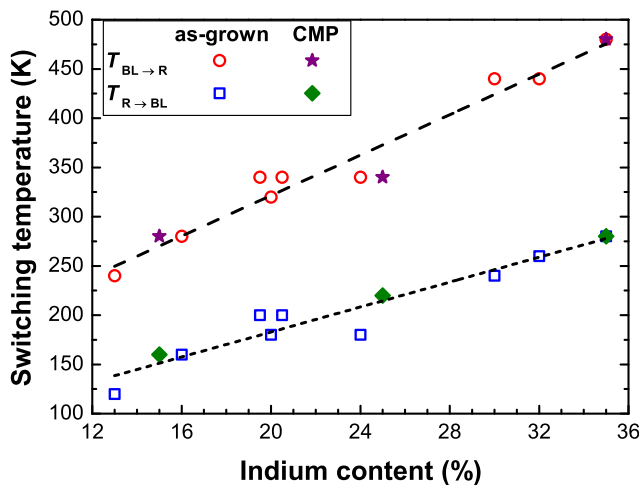


FIG. 3. Switching temperatures of the $(11\bar{2}2)$ InGaIn MQW samples grown on as-grown and CMP-templates as a function of In-content.

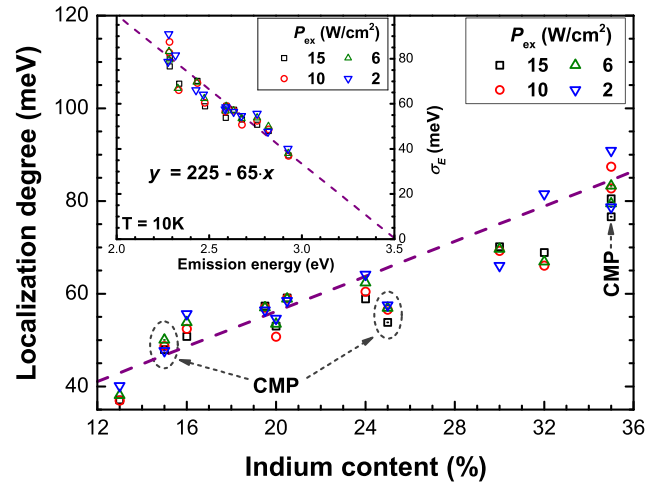


FIG. 4. The ELOC degree (σ_E) of the $(11\bar{2}2)$ InGaIn MQW samples grown on as-grown (open symbols) and CMP-templates (dot-centre symbols) as a function of In-content. The inset shows the ELOC degree as a function of the MQW emission energy measured at 10 K.

$(11\bar{2}2)$ $\text{In}_{0.2}\text{Ga}_{0.8}\text{N}$ MQW.²¹ Since the measurements were performed under the weak P_{ex} , the QCSE can be neglected. For the $(11\bar{2}2)$ samples studied here, the unchanged peak emission energies and σ_E values indicate that a strong ELOC exists in the samples. A similar finding has been previously reported for m -plane $\text{In}_x\text{Ga}_{1-x}\text{N}$ MQW samples ($5\% \leq x \leq 30\%$)¹⁸ though these samples grown on high-TDD high-BSF-density templates showed much less pronounced S-shaped behaviour compared to the samples studied here. The large σ_E value of the $(11\bar{2}2)$ samples studied here is believed to derive from the anisotropic growth on the $(11\bar{2}2)$ surface^{26,27,29} and the onset of relaxation in $(11\bar{2}2)$ nitrides.^{28,31} The strong ELOC in m -plane MQW¹⁸ and the $(11\bar{2}2)$ MQW samples studied here can be another reason that should be taken into account with the reduced polarization fields^{4,5} to explain why non-/semi-polar MQW structures have a much shorter radiative lifetime compared to polar MQW.^{4,12–14,20}

To investigate the Stokes-shift of the samples, PL spectra together with PLE absorption edge were measured at 10 K using the Xe-lamp excitation source ($P_{ex} \sim 10^{-5}$ W/cm²). The PLE measurements were performed with a detection energy fixed at each MQW peak emission energy. Figure 5(a) shows examples of 10 K PL spectra of two samples measured with $E_{ex} = 3.815$ eV. The GaN near-band-edge (NBE) luminescence at about 3.475 eV and GaN donor-acceptor-pair (DAP) at about 3.3 eV can be clearly seen, while the MQW NBE can be observed at about 2.6 eV and 2.7 eV. It should be noted that the FWHM value of the 10 K PL spectrum under the Xe-lamp excitation is comparable with the value obtained under the laser excitation, similar to a previous finding for $(11\bar{2}2)$ $\text{In}_{0.2}\text{Ga}_{0.8}\text{N}$ MQW.²¹

The PLE edge of the $(11\bar{2}2)$ InGaIn/GaN MQW samples was estimated using a sigmoidal fit^{32,33}

$$\alpha(E) = \alpha_0 \left(\frac{1}{1 + \exp\left(\frac{E_B - E}{\Delta E}\right)} \right), \quad (2)$$

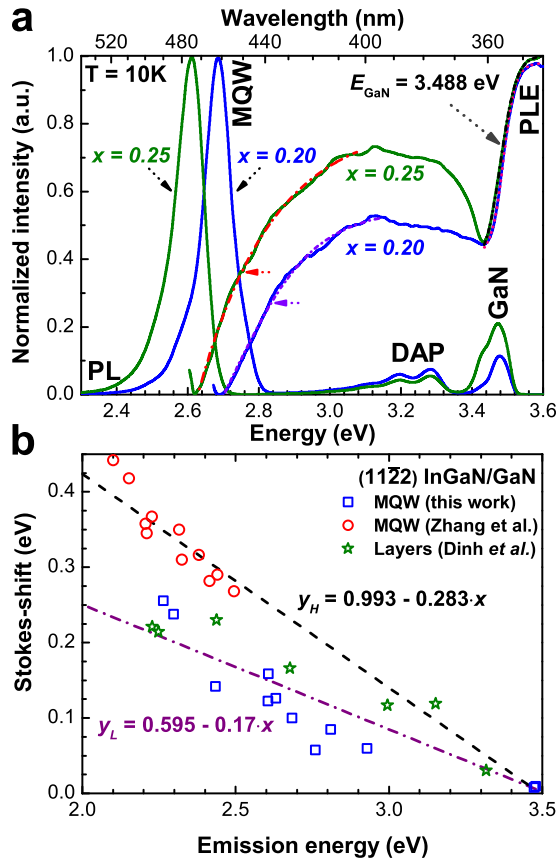


FIG. 5. (a) 10 K PL ($E_{ex} = 3.815$ eV, $P_{ex} \sim 10^{-5}$ W/cm²) and PLE measurements (solid-lines) of (11 $\bar{2}2$) InGaN MQW samples. Dashed/dotted-lines are the sigmoidal fitting using Eq. (2). (b) The Stokes-shift values of the samples (\square , this work) plotted as a function of the MQW emission energy at 10 K. The data points (\circ , at 12 K) by Zhang *et al.*¹⁴ and (\star , at 12 K) by Dinh *et al.*²⁸ are plotted for comparison. Lines ($y_{L,H}$) are two possible linear-fittings.

where α_0 is a constant; E_B is an “effective energy gap” of InGaN; ΔE is a broadening parameter that reflects the energy gap fluctuations resulting from In-Ga segregation, i.e., equivalent to the Urbach tailing energy. The Stokes-shift is defined as the energy difference between E_B and the MQW emission energy. The PLE edge value of GaN is estimated to be about 3.488 eV with the estimated Stokes-shift of 8–10 meV. The Stokes-shift values estimated for the InGaN/GaN MQW samples and GaN are shown in Fig. 5(b) together with previous results estimated for (11 $\bar{2}2$) InGaN MQW¹⁴ and (11 $\bar{2}2$) InGaN layers.²⁸ Despite the scattered data points, two possible trends (after linear fittings) can be observed, whereby the Stokes-shift values show linear dependence on emission energy, and tend to a zero value around the GaN bandgap of 3.5 eV. This is consistent with the change in the σ_E values shown in the inset of Fig. 4. It should be noted that the trend (y_H) is almost the same as a trend previously reported for polar InGaN MQW and layers.^{32,33} The Stokes-shift values estimated for the MQW samples (this work) and InGaN layers²⁸ are smaller than that of Zhang *et al.*,¹⁴ this might be due to differences in growth optimization. Though for the samples studied here, a different slope (y_L) has been observed compared to that of Zhang *et al.*,¹⁴ it somehow confirms their data whereby a “smaller” slope of Stokes-shift

has been found for (11 $\bar{2}2$) MQWs compared to polar MQWs.

Despite the large ELOC degree in the (11 $\bar{2}2$) MQW samples grown on low-TDD low-BSF-density (11 $\bar{2}2$) GaN templates, their IQE values ($IQE = I_{300K PL}/I_{10K PL}$ ³⁴) are low. The IQE values were, respectively, estimated to be about 30%, 20%, and 10% for the samples with $x = 13\%$, 25%, and 35%. The relative 10 K PL intensity of the samples follows a similar trend with the values of 1.0, 0.6, 0.24 estimated for the samples with $x = 13\%$, 25%, and 35%, respectively. The IQE values obtained for the samples grown on CMP-templates is only about 2%–5% higher than the samples grown on as-grown templates. These IQE values are much lower compared to polar samples grown under the same growth condition.²¹ One of the reasons for the low IQE values might be due to a high concentration of unintentional impurities in this (11 $\bar{2}2$) surface orientation;³⁵ another possible reason might be related to point defects.³⁶

IV. CONCLUSIONS

In summary, TD-PL measurements were carried out on (11 $\bar{2}2$) In_xGa_{1-x}N MQW samples ($0.13 \leq x \leq 0.35$) grown on high quality (11 $\bar{2}2$) GaN templates prepared on patterned *r*-plane sapphire substrates. A strong exciton localization (ELOC) was found in the samples which shows a linear dependence with In-content and emission energy, consistent with the Stokes-shift values. This strong ELOC was found to cause a blue-shift of the MQW exciton emission at temperature above 100 K. This temperature was found to increase with increasing In-content. Though the high quality templates were used, no improvement in optical efficiency was observed. This is attributed to a high concentration of unintentional impurities and point defects in the samples. It is therefore expected that the efficiency of (11 $\bar{2}2$) InGaN MQW can be significantly improved by lowering these concentrations.

ACKNOWLEDGMENTS

This work was financially supported by the EU-FP7 ALIGHT project, under Agreement No. FP7-280587. This work was also partially supported by the Programme for Research in Third Level Institutions (PRTLII) fourth and fifth cycles.

¹C. J. Humphreys, *MRS Bull.* **33**, 459 (2008).

²S. Chichibu, T. Azuhata, T. Sota, and S. Nakamura, *Appl. Phys. Lett.* **69**, 4188 (1996).

³E. Kuokstis, J. W. Yang, G. Simin, M. Asif Khan, R. Gaska, and M. S. Shur, *Appl. Phys. Lett.* **80**, 977 (2002).

⁴P. Waltereit, O. Brandt, A. Trampert, H. T. Grahn, J. Menniger, M. Ramsteiner, M. Reiche, and K. H. Ploog, *Nature* **406**, 865 (2000).

⁵A. E. Romanov, T. J. Baker, S. Nakamura, and J. S. Speck, *J. Appl. Phys.* **100**, 023522 (2006).

⁶W. H. Sun, J. W. Yang, C. Q. Chen, J. P. Zhang, M. E. Gaevski, E. Kuokstis, V. Adivarahan, H. M. Wang, Z. Gong, M. Su, and M. Asif Khan, *Appl. Phys. Lett.* **83**, 2599 (2003).

⁷Z. Vashaei, C. Bayram, P. Lavenus, and M. Razeghi, *Appl. Phys. Lett.* **97**, 121918 (2010).

⁸T. Detchprohm, M. Zhu, Y. Li, Y. Xia, C. Wetzel, E. A. Preble, L. Liu, T. Paskova, and D. Hanser, *Appl. Phys. Lett.* **92**, 241109 (2008).

⁹Y.-D. Lin, A. Chakraborty, S. Brinkley, H. C. Kuo, T. Melo, K. Fujito, J. S. Speck, S. P. DenBaars, and S. Nakamura, *Appl. Phys. Lett.* **94**, 261108 (2009).

- ¹⁰M. Funato, M. Ueda, Y. Kawakami, Y. Narukawa, T. Kosugi, M. Takahashi, and T. Mukai, *Jpn. J. Appl. Phys., Part 2* **45**, L659 (2006).
- ¹¹H. Sato, R. B. Chung, H. Hirasawa, N. Fellows, H. Masui, F. Wu, M. Saito, K. Fujito, J. S. Speck, S. P. DenBaars, and S. Nakamura, *Appl. Phys. Lett.* **92**, 221110 (2008).
- ¹²Y. Ji, W. Liu, T. Erdem, R. Chen, S. T. Tan, Z.-H. Zhang, Z. Ju, X. Zhang, H. Sun, X. W. Sun, Y. Zhao, S. P. DenBaars, S. Nakamura, and H. V. Demir, *Appl. Phys. Lett.* **104**, 143506 (2014).
- ¹³B. Liu, R. Smith, M. Athanasiou, X. Yu, J. Bai, and T. Wang, *Appl. Phys. Lett.* **105**, 261103 (2014).
- ¹⁴Y. Zhang, R. M. Smith, Y. Hou, B. Xu, Y. Gong, J. Bai, and T. Wang, *Appl. Phys. Lett.* **108**, 031108 (2016).
- ¹⁵P. G. Eliseev, P. Perlin, J. Lee, and M. Osinski, *Appl. Phys. Lett.* **71**, 569 (1997).
- ¹⁶D. Monroe, *Phys. Rev. Lett.* **54**, 146 (1985).
- ¹⁷M. Grünewald, B. Movaghar, B. Pohlmann, and D. Würtz, *Phys. Rev. B* **32**, 8191 (1985).
- ¹⁸C. Netzel, C. Mauder, T. Wernicke, B. Reuters, H. Kalisch, M. Heuken, A. Vescan, M. Weyers, and M. Kneissl, *Semicond. Sci. Technol.* **26**, 105017 (2011).
- ¹⁹T. Langer, H.-G. Pietscher, F. A. Ketzer, H. Jönen, H. Bremers, U. Rossow, D. Menzel, and A. Hangleiter, *Phys. Rev. B* **90**, 205302 (2014).
- ²⁰R. Ivanov, S. Marcinkevičius, Y. Zhao, D. L. Becerra, S. Nakamura, S. P. DenBaars, and J. S. Speck, *Appl. Phys. Lett.* **107**, 211109 (2015).
- ²¹D. V. Dinh, S. Presa, P. P. Maaskant, B. Corbett, and P. J. Parbrook, *Semicond. Sci. Technol.* **31**, 085006 (2016).
- ²²See <http://www.alight-project.eu> for the ALIGHT project description.
- ²³F. Brunner, U. Zeimer, F. Edokam, W. John, D. Prasai, O. Krüger, and M. Weyers, *Phys. Status Solidi B* **252**, 1189 (2015).
- ²⁴D. V. Dinh, M. Akhter, S. Presa, G. Kozłowski, D. OMahony, P. P. Maaskant, F. Brunner, M. Caliebe, M. Weyers, F. Scholz, B. Corbett, and P. J. Parbrook, *Phys. Status Solidi A* **212**, 2196 (2015).
- ²⁵C. Q. Chen, M. E. Gaevski, W. H. Sun, E. Kuokstis, J. P. Zhang, R. S. Q. Fareed, H. M. Wang, J. W. Yang, G. Simin, M. A. Khan, H.-P. Maruska, D. W. Hill, M. M. C. Chou, and B. Chai, *Appl. Phys. Lett.* **81**, 3194 (2002).
- ²⁶S. Ploch, T. Wernicke, D. V. Dinh, M. Pristovsek, and M. Kneissl, *J. Appl. Phys.* **111**, 033526 (2012).
- ²⁷D. V. Dinh, D. Skuridina, S. Solopow, M. Frentrop, M. Pristovsek, P. Vogt, M. Kneissl, F. Ivaldi, S. Kret, and A. Szczepańska, *J. Appl. Phys.* **112**, 013530 (2012).
- ²⁸D. V. Dinh, F. Oehler, V. Z. Zubialevich, M. J. Kappers, S. N. Alam, M. Caliebe, F. Scholz, C. J. Humphreys, and P. J. Parbrook, *J. Appl. Phys.* **116**, 153505 (2014).
- ²⁹L. Lymperakis and J. Neugebauer, *Phys. Rev. B* **79**, 241308 (2009).
- ³⁰Y. P. Varshni, *Physica* **34**, 149 (1967).
- ³¹E. C. Young, F. Wu, A. E. Romanov, A. Tyagi, C. S. Gallinat, S. P. DenBaars, S. Nakamura, and J. S. Speck, *Appl. Phys. Express* **3**, 011004 (2010).
- ³²K. P. O'Donnell, R. W. Martin, and P. G. Middleton, *Phys. Rev. Lett.* **82**, 237 (1999).
- ³³R. W. Martin, P. G. Middleton, K. P. O'Donnell, and W. Van der Stricht, *Appl. Phys. Lett.* **74**, 263 (1999).
- ³⁴Y. Narukawa, Y. Kawakami, S. Fujita, and S. Nakamura, *Phys. Rev. B* **59**, 10283 (1999).
- ³⁵S. C. Cruz, S. Keller, T. E. Mates, U. K. Mishra, and S. P. DenBaars, *J. Cryst. Growth* **311**, 3817 (2009).
- ³⁶S. F. Chichibu, A. Uedono, T. Onuma, S. P., U. K. Mishra, J. S. Speck, and S. Nakamura, *Mater. Sci. Forum* **590**, 233 (2008).